Electronic Supplementary Information

New strategy for engineering hierarchical porous carbon-anchored Fe single-atom electrocatalyst and the insights into its bifunctional catalysis for flexible rechargeable Zn-air battery

Cheng Du,[a,c] *Yijing Gao,*[b] *Jianguo Wang,*[b,*] *and Wei Chen,*[a, c*]

[a] State Key Laboratory of Electroanalytical Chemistry, Changchun Institute of Applied Chemistry, Chinese Academy of Sciences, Changchun, Jilin 130022, China

[b] Institute of Industrial Catalysis, State Key Laboratory Breeding Base of Green-Chemical Synthesis Technology, College of Chemical Engineering, Zhejiang University of Technology, Hangzhou 310032, P.R. China

[c] University of Science and Technology of China, Hefei, Anhui 230029, P.R.China

* Corresponding author. E-mail: jgw@zjut.edu.cn; weichen@ciac.ac.cn

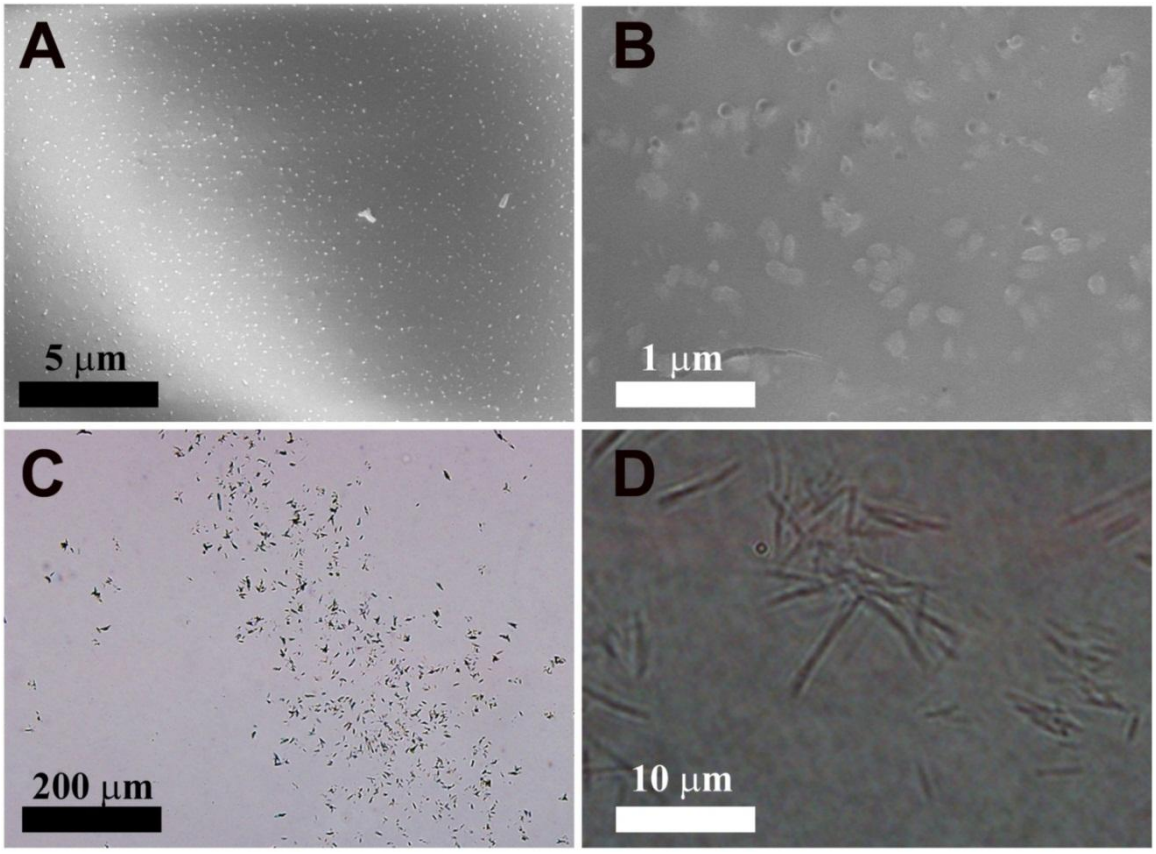

Fig. S1 (A-B) SEM images of ferric nitrate nanocrystals after the confined recyrstallization with a size of about 200 nm; (C-D) Optical microscope images of ferric nitrate salt with a size of few micrometers. Iron nitrate nonahydrate salt is easy to be decomposed under the electron beam during SEM measurement and clear image cannot be obtained; therefore optical microscope was used to characterize the size.

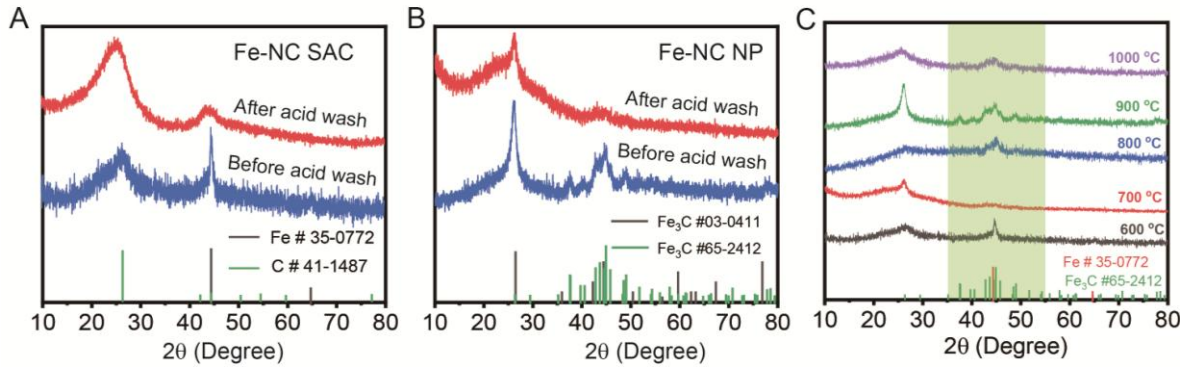

Fig. S2 (A-B) XRD patterns of Fe-NC SAC (A) and Fe-NC NP (B) before and after acid washing; (C) XRD patterns of Fe-NC NP samples prepared under different temperatures.

In the XRD pattern of Fe-NC SAC before acid washing (Figure S2A), two obvious sharp peaks of Fe at 44^{o} and 65^{o} (#06-0696) are observed. However, there are only two broad peaks at 26^{o} and 42^{o} of carbon (#41-1487) existing in the XRD spectrum of Fe-NC SAC after acid washing, indicating the successful removal of Fe NPs by acid washing. For the Fe-NC NP, a group peaks of Fe_3C (#65-2412) and a sharp peak at 27^{o} belonging to Fe_3C (#03-0411) apparently appear in the XRD pattern of Fe-NC NP before acid washing. After acid washing, all of these diffraction peaks of Fe_3C are weakened but still exist in the XRD pattern. Such result suggests the presence of Fe_3C NPs in the final Fe-NC NP sample, agreeing well with the HRTEM results. What should be noted that, the peaks of carbon are broad due to its amorphousness while the Fe or Fe_3C are well crystallized with sharp diffraction peaks, which is an important basis to distinguish them in the overlaped signals.

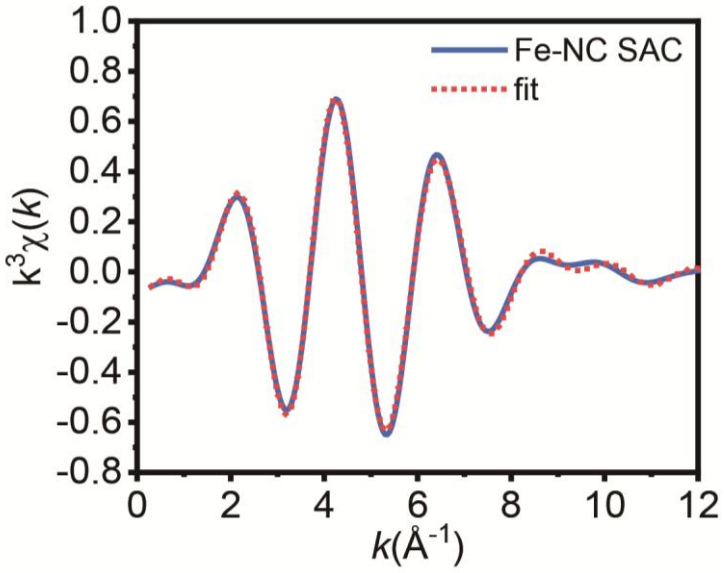

Fig. S3 The fitting curve of Fe-NC SAC in k space.

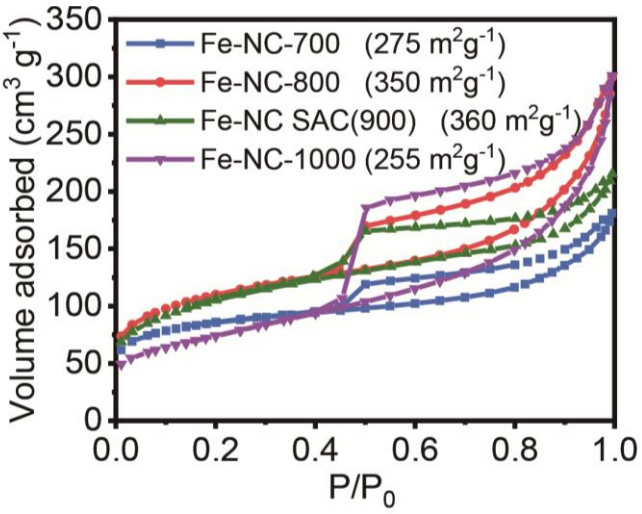

Fig. S4 Nitrogen adsorption–desorption isotherms of Fe-NC samples prepared under different temperatures.

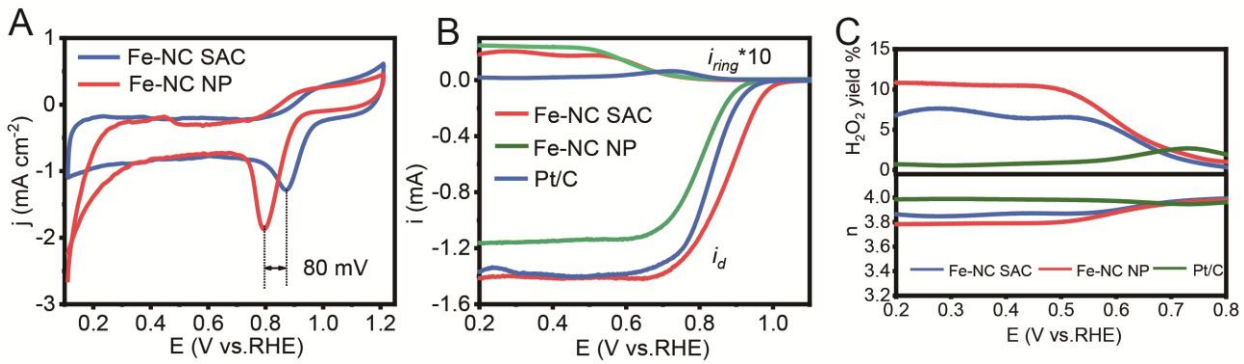

Fig. S5 (A) CV curves of Fe-NC SAC and Fe-NC NP in O_2-saturated 0.1 M KOH, scan rate: 20 mV s^{-1}; (B) RRDE LSV curves of ORR on the Fe-NC SAC, Fe-NC NP and Pt/C at 1600 rpm, scan rate: 5 mV s^{-1}; (C) H_2O_2% and n numbers calculated from the LSV curves in (B).

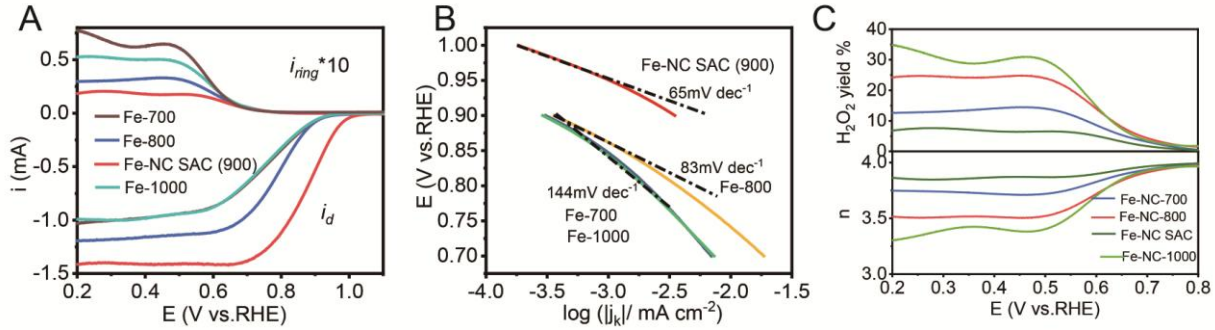

Fig. S6 (A-C) LSV curves of ORR on RRDE under 1600 rpm (A), Tafel curves (B), and calculated H_2O_2% and n numbers (C) on the Fe-NC-T samples, scan rate: 5 mV s^{-1}.

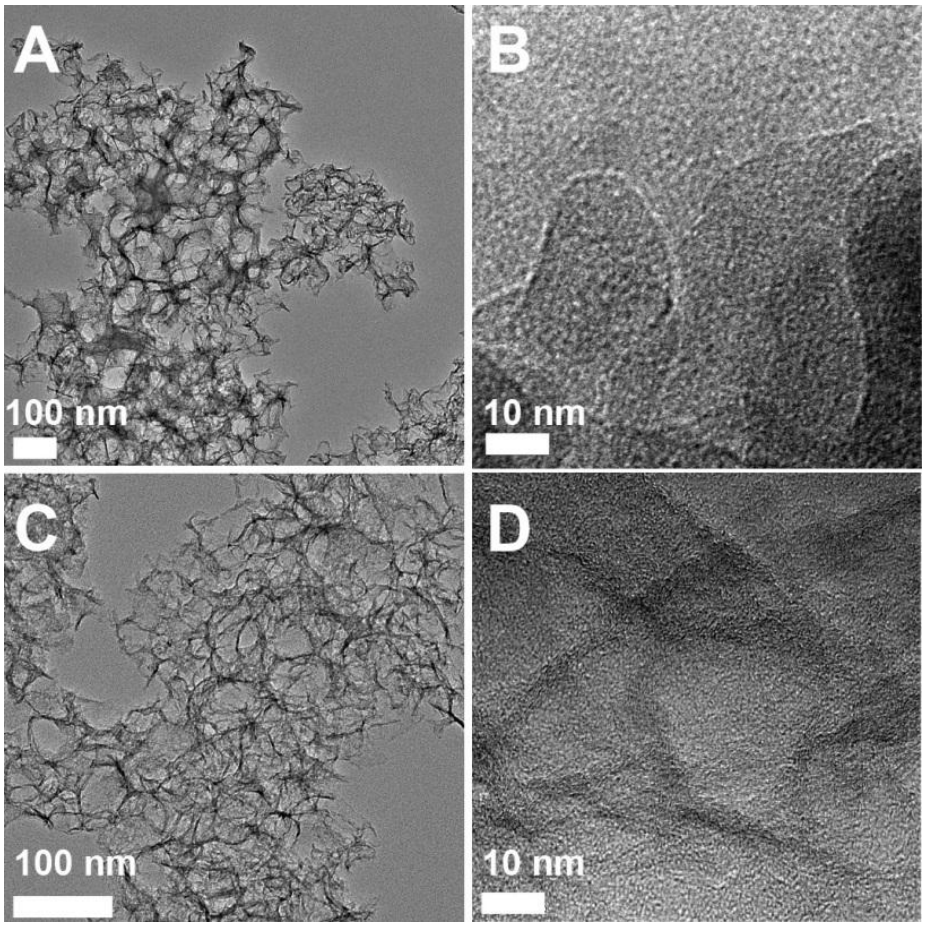

Fig. S7 TEM images of Fe-NC SAC after ADT of ORR (A-B) and OER (C-D).

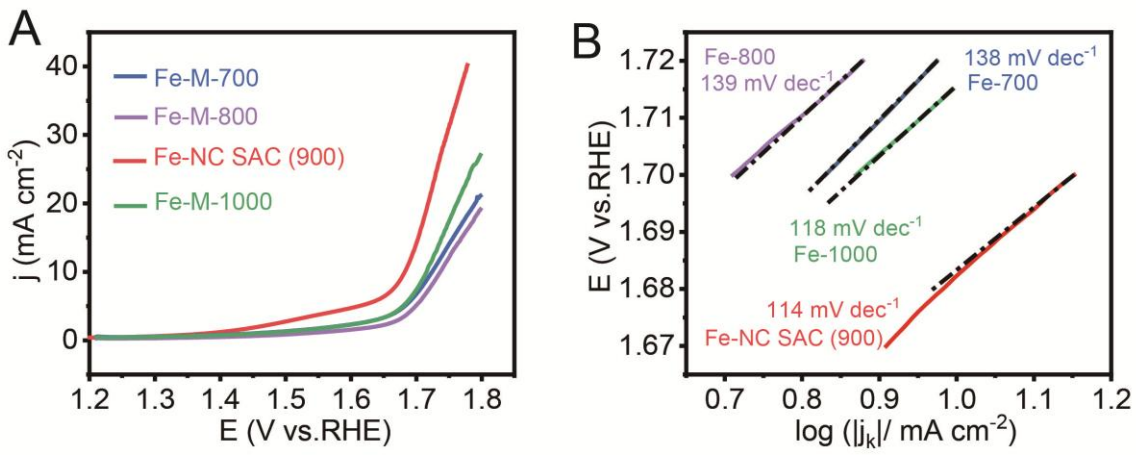

Fig. S8 (A) LSV curves of OER on different samples under 1600 rpm with a scan rate of 5 mV s^{-1}. (B) Tafel plots of OER on the Fe-NC-T samples.

Table. S1 Fitted EXAFS parameters at the Fe K-edge for Fe-NC SAC

Sample	Shell	N [a]	R (Å) [b]	σ^2 (Å^2 ·10^3) [c]	$\Delta E0$ (eV) [d]	R factor (%)
Fe-NC SAC	**Fe-N**	**4.7**	**1.98**	**8.6**	**-1.1**	**1.1**

[a] N: coordination numbers; [b] R: bond distance; [c] σ^2: Debye-Waller factors; [d] ΔE_0: the inner potential correction. R factor: goodness of fit.

Table. S2 The configurations and contents of different types of N in the Fe-NC SAC from XPS data.

	Pyridinic N (398.7eV)	**Fe-Nx (399.7eV)**	**pyrrolic N (400.8 eV)**	**graphitic N (402.3 eV)**	**oxidized N (403.5eV)**	**Total N contant**
Fe-NC SAC	39%	12%	27%	16%	6%	1.66%

Table. S3 Pore structure data of the prepared samples obtained from the nitrogen isothermal adsorption/desorption measurements.

	Fe-NC-700	Fe-NC-800	Fe-NC SAC	Fe-NC-1000	Fe-NC NP
S-total (cm^2g^{-1})	275	350	360	255	180
S-micro (cm^2g^{-1})	121	65	98	31	50
S-meso (cm^2g^{-1})	153	291	265	229	130
V-total (cm^3g^{-1})	0.25	0.3	0.39	0.38	0.27
V-micro (cm^3g^{-1})	0.06	0.04	0.05	0.01	0.03
V-meso (cm^3g^{-1})	0.19	0.26	0.34	0.37	0.24
Porosity	0.33	0.38	0.44	0.43	0.35
Micro-porosity	0.08	0.05	0.06	0.01	0.04
Meso-porosity	0.25	0.33	0.38	0.42	0.31

* The S represents the specific surface area; V represents the specific volume.
The porosity was calculated based on the following equation:

$$Porosity = \frac{Pore\ volume}{Pore\ volume + Carbon\ volume};$$

Here, the intrinsic density of carbon is 1.99 g cm^{-3}. (Chem. Eng. J. 2010, 160, 398.)

Table. S4 Comparison of the electrocatalytic activities of the reported bifunctional catalysts and the materials prepared in this work for the ORR/OER

Catalyst	$E_{1/2}$	E_{10}	E_{10} - $E_{1/2}$	Electrolyte	Ref
Fe-NC SAC	***0.88***	***1.68***	***0.8***	***0.1M KOH***	***This work***
Fe-NC NP	0.79	1.76	0.97	0.1M KOH	This work
Pt/C+RuO_2	0.83	1.73	0.9	0.1M KOH	This work
Co-POC *(SAC)*	0.83	1.70	0.87	0.1M KOH	Adv. Mater. 2019, 1900592
Co-N_x-C *(SAC)*	0.79	1.74	0.95	0.1M KOH	Adv. Mater. 2017, 1703185
Co-N,B-CSs *(SAC)*	0.83	1.66	0.83	0.1M KOH	ACS Nano 2018, 12, 1894
FeN_x-PNC *(SAC)*	0.86	1.64	0.78	0.1M KOH	ACS Nano 2018, 12, 2, 1949-1958
NCNF-1000	0.82	1.84	1.02	0.1M KOH	Adv. Mater. 2016, 28, 3000
N-GCNT/FeCo-3	0.92	1.73	0.81	0.1M KOH	Adv. Energy Mater. 2017, 1602420
CuS/NiS_2 INs	0.73	1.52	0.79	0.1M KOH	Adv. Funct. Mater. 2017, 1703779
(NCNT) arrays	0.81	1.65	0.84	0.1M KOH	Nano Energy 2017,37, 98–107
DN-CP@G	0.8	1.79	0.99	0.1M KOH	Adv. Energy Mater. 2018, 1703539
CoSx@PCN/rGO	0.78	1.57	0.79	0.1M KOH	Adv. Energy Mater. 2018, 8, 1701642
Ni–MnO/rGO	0.78	1.6	0.82	0.1M KOH	Adv. Mater. 2018, 30, 1704609
Pd@PdO–Co_3O_4	0.73	1.54	0.81	0.1M KOH	Adv. Energy Mater. 2017, 1702734
Ni_3FeN	0.78	1.59	0.81	0.1M KOH	Nano Energy 2017,39, 77–85
$MnCo_2O_4$	0.8	1.63	0.83	0.1M KOH	Angew. Chem. 2017, 129, 15173
$Co_3FeS_{1.5}(OH)_6$	0.72	1.59	0.87	0.1M KOH	Adv. Mater. 2017, 1702327
Meso-CoNC@GF	0.87	1.66	0.79	0.1M KOH	Adv. Mater. 2017, 1704898
$CoO_{0.87}S_{0.13}$/GN	0.83	1.59	0.76	0.1M KOH	Adv. Mater. 2017, 1702526
Mo–N/C@MoS_2	0.81	1.62	0.81	0.1M KOH	Adv. Funct. Mater. 2017, 1702300
CoZn-NC-700	0.84	1.62	0.78	0.1M KOH	Adv. Funct. Mater. 2017, 1700795
Ni_3Fe/N-C sheets	0.78	1.62	0.84	0.1M KOH	Adv. Energy Mater. 2017, 7, 1601172
NiCo/PFC aerogels	0.79	1.63	0.86	0.1M KOH	Nano Lett. 2016, 16, 6516−6522

* $E_{1/2}$ refers to the half wave potential of ORR;

E_{10} refers to the OER potential value at current density of 10 mA cm^{-2}.

Table. S5 Fe content in the Fe-NC SAC after ADT from ICP-AES result.

	Before ADT	**ORR ADT**	**OER ADT**
1st test	1.55 wt%	1.4 wt%	1.5 wt%
2nd test	1.45 wt%	1.5 wt%	1.4 wt%

The little difference should be ascribed to the instrumental error. Apparently, the content of Fe almost have no loss after ADT, indicating the excellent stability of Fe SAC.